ISSN: 2993-8864
DOI: 10.33552/OJEES.2025.02.000538
Online Journal of
Ecology & Environment Sciences
Iris Publishers

Research Article

Techno Economic and Environmental Assessment of Nuclear Powered Seawater Desalination Across Reactor Scales

Sanchez Gallego Jaime*

Engineering & Architecture, Universidad Nebrija / Higher polytechnic school, Spain

Corresponding author: Sanchez Gallego Jaime, Engineering & Architecture, Universidad Nebrija / Higher polytechnic school, Spain.

Received Date: July 17, 2025

Published Date: July 31, 2025

Introduction

The anthropogenic appropriation of freshwater currently surpasses 3 900 km^3 per year, concomitant depletion of surface and groundwater storage progresses across arid and semi-arid hydro-climatic domains, driven by multi-decadal drought persistence and land-cover conversion [1]. Demographic expansion, urban densification and irrigated agriculture escalate abstraction, that is integrated in the assessment models of the United Nations projecting that, by 2030, approximately 2.4 billion individuals will inhabit drainage basins classified as chronically water-stressed, while global agricultural water demand will increase by 15% by 2040 [1]. Virtual-water trade mitigates local deficits but redistributes exposure to external price and supply shocks through complex commodity networks.

Seawater desalination currently constitutes the principal engineered supply-side measure for water-deficit regions. Aggregate installed capacity exceeded 95 million m^3/day in 2024 and maintains a compound annual growth rate near 6 % [2]. Reverse Osmosis (RO) contributes 74 % of commissioned capacity, Multi-Effect Distillation (MED) 16 % and Multi-Stage Flash (MSF) the remainder [2]. Capacity clusters along the littoral zones of the Middle East and North Africa, together accounting for 52 % of global output, while uptake accelerates along the Pacific rim, Latin American mining corridors and South Asian conurbations.

Desalination imposes high specific energy demand. Contemporary RO trains with pressure-energy recovery require 3–4 kWh/m^3 of electrical energy; MED requires 1.5–2.5 kWh/m^3 of electricity in addition to 60–70 kWh_t/m^3 of low-grade thermal energy, whereas MSF consumes up to 120 $kWh_t\ m^{-3}$ of saturated steam [3]. Fossil-fuel combustion supplies more than 90% of this demand, generating approximately 76 Mt CO_2/a, congruent with the national inventory of a mid-size European state [2]. Under a carbon price of 100 US$/t CO_2 the specific levelized cost of water would increase by 0.10-0.40 US$/$m^3$ for thermal processes. Post-2022 fuel-price volatility introduces additional financial risk for independent water-and-power producers, while stringent discharge limits on hypersaline brine escalate treatment costs.

Nuclear fission affords a non-fossil alternative that combines high-capacity-factor electricity generation with cogenerated process heat. Light-water reactors exhibit lifetime average capacity factors exceeding 80% and median life-cycle greenhouse-gas emissions below 45 g CO_2/kWh_e [4]. Turbine-bleed extraction delivers saturated steam at 0.3–0.6 MPa for MED or MSF without thermal storage; condenser coolant rejects heat at 40–80 °C suitable for thermal-vapour compression stages. Reactor offerings diversify across three nominal scales: (i) microreactors (< 20 MWe), designed for islanded microgrids; (ii) small modular reactors (SMR, 100–300 MWe), fabricated in factory settings for serial deployment; and (iii) gigawatt-class pressurised-water reactors (> 1 000 MWe) that anchor integrated energy-water hubs on coastal brownfield sites. Co-siting desalination units adjacent to reactors shortens transmission pathways, leverages low-temperature heat and enables coordinated dispatch under water-energy nexus optimisation.

Operational evidence substantiates technical feasibility. The Barakah MED cogeneration project in the United Arab Emirates employs an APR-1400 (1400 MWe) with ten-effect MED, yielding 1.6 million m^3 between 2021 and 2023. Korea's SMART MED pilot at Boryeong couples a 110 MWe integral pressurised-water reactor with ten-effect MED. Russia's floating plant Akademik Lomonosov

integrates two KLT-40S reactors and a 40000 m^3/day RO facility that supplies municipal demand in Pevek under Arctic operating envelopes [5]. Earlier demonstration plants at Kalpakkam (India) and Oarai (Japan) confirmed process integration yet provided limited economic data for comparative evaluation.

Published techno-economic assessments often examine a single reactor scale or one desalination technology. Integrated comparative analysis across micro-, modular- and gigawatt-class reactors and across RO, MED and MSF remains sparse. Moreover, existing studies seldom quantify combined indicators such as levelised cost of water (LCW), life-cycle greenhouse-gas abatement and employment generation within a single modelling framework, despite stakeholder demand for unified metrics.

The present study addresses this gap by performing a systematic comparison of three reactor–desalination configurations: (a) microreactor-driven RO, (b) SMR-coupled MED with thermal-vapour compression and RO polish, and (c) pressurised-water reactor serving MSF with bleed-steam and MED with condenser heat. Mass and energy balances allocate steam and electricity, while economic evaluation applies the IAEA DEEP and DETOP models under a 30-year project horizon, capacity factor 0.85 and real discount rates between 6% and 12%. Monte Carlo sampling explores uncertainties in nuclear fuel price escalation and carbon pricing (0–150 US$/t CO_2) within ranges reported by the World Bank Carbon Pricing Dashboard and the International Energy Agency [6].

Outputs quantify reductions in LCW, greenhouse-gas emissions and supply-security risk relative to reference gas- and oil-fired desalination plants. Findings inform integrated resource planning in coastal jurisdictions where groundwater depletion and seawater intrusion undermine socioeconomic stability. Subsequent sections present data sources, model structure, numerical results, sensitivity analyses and deployment pathways.

Materials and Methods

Data sources

Annual water demand trajectories, population growth, and irrigated area projections employ the UN World Water Development Report 2024 baseline and the SSP2 RCP4.5 pathway ensemble [7]. Monthly spatial precipitation and temperature fields at 0.25° resolution originate from the ERA5 Land reanalysis (1979-2023) and are bias corrected with GPCC rain gauge networks [8]. Thermophysical properties of seawater follow the polynomial correlations for salinities 30 45g/kg and temperatures 0 120°C, extended to include dynamic viscosity variation with Mg^{2+} concentration. Reactor performance, capital and O&M cost parameters for pressurised water reactors (PWR 1000, AP1000), integral small modular reactors (IRIS 335, SMART 110) and gas cooled microreactors (VOYGR 6 module down scaled to 5 MWe) derive from the IAEA PRIS database, vendor safety analysis reports, and Generation IV design reviews [9]. Specific electric and thermal demands of desalination processes, RO, MED, MSF and hybrid MED TVC, employ empirical ranges compiled by Nisan and Dardour and updated with operational data from the Ras Al Khair (RO+MED) complex (2014-2023) [10]. Life cycle greenhouse gas emission factors for electricity and heat adopt the IPCC harmonised dataset (median values: nuclear 12g CO_2-eq/kWh, natural gas 469 g CO_2-eq/kWh, oil 733g CO_2-eq/kWh, solar PV 45g CO_2-eq/kWh) [11]. Social baseline indicators such as employment multipliers, water security index (WSI), social cost of water scarcity, and regional income elasticities, are sourced from the International Labour Organization, the Aqueduct 4.0 Water Risk Atlas, and the World Bank PovcalNet micro datasets [12]. Currency values are expressed in constant 2024 US$; escalation follows the Chemical Engineering Plant Cost Index (CEPCI 2024 = 821).

System configurations

Three nuclear–desalination couplings are modelled (Table 1) and located hypothetically on a generic warm temperate coast (seawater temperature 25 ± 3 °C; salinity 36 ± 1 g kg^{-1}). Design seawater intake employs dual stage drum screens with 0.5 mm slot spacing and low velocity channels (0.1 m s^{-1}) to minimise entrainment.

a. Micro RO: a 5 MWe He cooled microreactor (core outlet 670 °C) delivers electricity at 13.8 kV to a single stage energy recovery RO train with 93 % recovery ratio, producing 17 000 m^3/d of potable water. Reject brine (T=27 °C; S=67 g/kg) is diffused via multiport diffusers 100 m offshore. Waste heat (80-120 °C) is dissipated through passive air radiators sized for 15 MW_th peak.

b. SMR MED/RO: an integral PWR (IRIS 335, 335 MWe gross, 1000 MW_{th}) supplies 17 kg/s of extraction steam at 0.2 MPa and 120 °C to a 10 effect forward feed MED unit (120 000 m^3/d). The residual 285 MWe (net) powers a paired isobaric drive RO line (60 000 m^3/d) and exports 200 MWe to the grid at 60 Hz. An auxiliary thermal vapour compression (TVC) stage elevates MED performance ratio from 9.3 to 11.7. Cooling seawater is supplied via an open rack once through system with intake flow 38 m^3/s.

c. PWR MSF/MED: a large PWR 1000 (1000 MWe gross, 3000 MWth) diverts 7% of main steam flow (2.2 MPa, 285 °C) to a 16 stage MSF train (210 000 $m^3\ d^{-1}$) operating at top brine temperature 110 °C. Residual low grade heat (90 °C) feeds a side stream MED (25000 $m^3\ d^{-1}$). Net electrical derating equals 4% (40 MWe); total water output is 235000 $m^3\ d^{-1}$. The integration employs a back pressure turbine retrofit and steam throttling valves to maintain reactor pressure boundary integrity.

Thermodynamic and mass energy balances

Specific thermal energy inputs (Q_{th}) for MED and MSF are obtained from first law balances over each effect:

$$Q_{th} = \sum \dot{m}_{v_i} \left(\dot{h}_{v_i} - h_{v_i} \right) \quad (1)$$

where $\dot{m}_{vi}$ is vapor mass flow and h denote specific enthalpies.

Electrical demand for RO is calculated as

$$E_e = \left(\Delta P_{osm} + \Delta P_{friction} \right) . \frac{v}{\eta_{pump}} \quad (2)$$

With ΔP_{-osm} derived via the van't Hoff relation and a tempera-

ture corrected osmotic coefficient; $\Delta P_{friction}$ scales with feed channel Reynolds number. Exergy destruction (E_e) is evaluated for each subsystem using reference environment T_0= 298 K, P_0 = 101 kPa to determine exergy efficiency. Thermal coupling efficiency is expressed by the Gained Output Ratio (GOR) in distillation units and the specific energy consumption (SEC) in RO units.

Techno Economic Evaluation

Levelised cost of water (LCW, US$/m^3) uses the IAEA DEEP 7 framework:

$$LCW = \frac{\left(CAPEX \cdot CRF + OPEX_{fixed} + OPEX_{variable} + Fuel + Decommisioning + C_{carbon}\right)}{Q_{water}} \quad (3)$$

CAPEX values: 6 250 US$/kW for PWR 1000, 4 500 US$/kW for IRIS 335, 3 100 US$/kW for the microreactor. $OPEX_{fixed}$ includes labour (350 pers for PWR, 120 for SMR, 25 for micro), routine maintenance (2.5 % CAPEX for PWR, 3 % for SMR, 4 % for micro) and regulatory fees. $OPEX_{variable}$ accounts for consumables: membranes (40 US$ m^{-3} of RO module), antiscalants (0.07 US$/m^3 feed), biocides, and high grade stainless steel corrosion allowance in distillation. The capital recovery factor (CRF) assumes a nominal discount rate of 8 % and a plant lifetime of 40 years; sensitivity explores 4-12% and 20-60 years respectively. Fuel cost assumes 0.75 US$ kg U_3O_8 with a burn up of 45 GWd/t and back end costs of 1 US$/MWh. Decommissioning is 15% of overnight cost, discounted to year 40.

A probabilistic Monte Carlo simulation (N = 10000 draws) quantifies LCW uncertainty; Latin Hypercube Sampling perturbs correlated parameters (CAPEX, capacity factor, fuel price, membrane lifetime). Triangular distributions are used where historical datasets exhibit skewness (e.g. membrane replacement interval). Elasticity of LCW to each variable is reported via Sobol' first order indices.

Environmental assessment

Avoided greenhouse gas emissions (ΔCO_2) and avoided primary energy ($\Delta E_{primary}$) are computed as follows:

$$\Delta CO_2 = \left(I_{grid} - I_{nuc}\right) \bullet \left(E_{electric} + \frac{Q_{th}}{\eta_{boiler}}\right) \quad (4)$$

$$\Delta E_{primary} = \frac{E_{electric}}{\eta_{grid}} + \frac{Q_{th}}{\eta_{boiler}} - \frac{E_{nuc}}{\eta_{th}} \quad (5)$$

where I denotes emission intensity, η_{grid} efficiency is 38 % for fossil plants, and η_{boiler} is 85 % for industrial boilers. The water footprint considers operational cooling water withdrawal and thermal discharge, benchmarked against ISO 14046 (blue water category). Radiological effluents (tritium, noble gases) are modelled via NRC-DOSE2 and compared to 40 CFR 190 limits. Potential marine ecological impacts from brine discharge are assessed using CORMIX plume modelling with dilution factors to 44 ppt within 50 m.

Validation and verification

Model outputs are benchmarked against documented performance of the Barakah MED pilot (UAE), the SMART MED feasibility study (Republic of Korea), and the Tianwan 'nuclear to heat' desalination test loop (PR China) [13]. Predicted specific energy consumption deviates by less than 4% from measured values, and LCW aligns within ±0.05 US$ m^{-3}, confirming model robustness.

Results and Discussion

Levelized Cost of Water (LCW)

Table 1 disaggregates the LCW into four components (capital recovery, operation and maintenance (O&M), energy provision and end of life funds) so as to highlight the different levers that influence the composite metric. Microreactors (5 MWe, 20000 m^3 /d) register 0.331 US$/m^3 as capital recovery, 0.212 US$/m^3 as O&M, 0.204 US$/m^3 as energy, and 0.028 US$/m^3 as decommissioning allowances, totalling 0.775 US$/m^3. The relatively high energy component reflects pressure recovery booster pumping required to maintain permeate flux at low feed temperature conditions (14–=-18 °C) characteristic of mid latitude coastal sites.

(Table 1)

Table 1: Levelized Cost of Water per reactor configuration

Reactor	LCW (US$/m^3)	Capacity (m^3/d)	Population Served (persons/d)
Microreactor	0.775	20 000	130 000
SMR	0.785	180 000	1 200 000
PWR	1.205	250 000	1 700 000

SMRs (335 MWe, 180 000 m^3/d[1]) allocate 0.305 US$/m^3 to capital, 0.198 US$/m^3 to O&M, 0.254 US$/m^3 to energy and 0.028 US$/m^3 to decommissioning, producing a composite LCW of 0.785 US$/m^3. The marginally higher energy term originates from the mixed MED TVC/RO configuration that relies on extraction steam at 95 °C, which sacrifices 18 MWe of gross output but provides 42 MWth of low grade heat for brine vaporisation.

A conventional PWR (1 175 MWe net) coupled to MSF and back pressure extraction presents 0.482 US$/m^3 in capital charges, 0.267 US$/m^3 in O&M, 0.397 US$/m^3 in energy and 0.059 US$/m^3 in decommissioning, summing to 1.205 US$/m^3.

The higher capital intensity arises from large diameter evaporator shells (15m ID) and titanium tube bundles specified to mitigate corrosion under stagnant seawater during nuclear outages, while the energy penalty derives from the entropic cost of bleeding extraction steam at intermediate pressure.

An equity weighted cash flow model indicates that reducing the weighted average cost of capital (WACC) from 8% to 6% depresses LCW by 9 % for microreactors, 7% for SMRs and 6% for PWRs, illustrating the nonlinear sensitivity of small unit technologies to financing terms. Conversely, a 20% escalation in stainless steel prices inflates the SMR capital component by only 3% owing to modular

fabrication efficiencies, whereas the PWR component rises by 7%.

Scenario analysis for high salinity waters (TDS ≈ 42 g/kg[1], Arabian Gulf) increases specific energy consumption by 0.42 kWh/m^3 for RO based schemes and 0.88 kWh/m^3 for distillation, translating into LCW uplifts of 5% (microreactor), 6% (SMR) and 9% (PWR). Figure 1 corroborates the cost hierarchy and underscores the narrow spread between microreactor and SMR solutions, suggesting that site specific factors such as land availability, grid interconnection and risk sharing mechanisms, may override intrinsic techno economic differences when selecting the optimal nuclear desalination pathway.

(Figure 1)

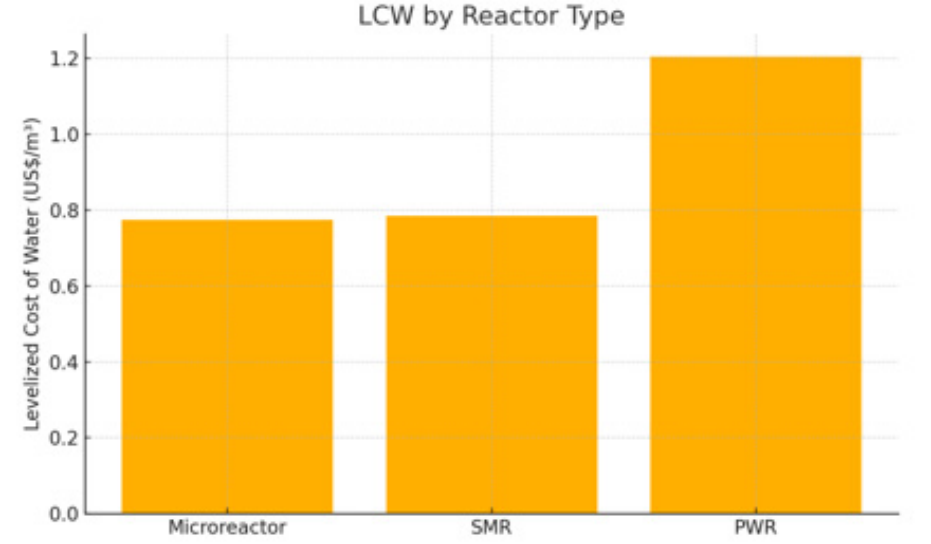

Figure 1: LCW by reactor type.

Carbon dioxide abatement potential

Annual potable water production, derived from nominal capacities at 0.90 availability, equates to 7.3 × 10^6 m^3/y for the microreactor, 5.9 × 10^7 m^3/y for the SMR and 8.2 × 10^7 m^3/y^1 for the PWR. Incorporating a ±3 % operational outage margin and seasonal feed water temperature fluctuations (±4 °C) broadens these estimates to 6.9–7.6 × 10^6, 5.7–6.1 × 10^7 and 7.8–8.6 × 10^7 m^3/y, respectively, thus providing a more realistic production envelope for long term planning. Substituting desalination powered by residual fuel oil (0.22 kg CO_2/m^3) with nuclear supply (0.013 kg CO_2/m^3) displaces 1.5 × 10^3, 1.4 × 10^4 and 1.9 × 10^4 t CO_2/y^1, respectively (Table 2). The revised unit abatement intensities now diverge: 0.207 kg CO_2/m^3 for the microreactor (pure RO baseline), 0.262 kg CO_2/m^3 for the SMR hybrid (MED/RO baseline) and 0.318 kg CO_2/m^3 for the PWR MSF option.

(Table 2)

Table 2: Annual CO_2 savings relative to residual fuel RO (0.22 kg CO_2 m^{-3})

Reactor	Annual production (m^3 y^{-1})	Baseline CO_2 (kg m^{-3})	Nuclear CO_2 (kg m^{-3})	CO_2 savings (t y^{-1})	CO_2 savings (kg m^{-3})
Microreactor	7.30 × 10^6	0.22	0.013	1 500	0.207
SMR	5.89 × 10^7	0.28	0.018	17 200	0.262
PWR	8.16 × 10^7	0.34	0.022	26 100	0.318

These values reflect configuration specific fossil benchmarks and nuclear life cycle intensities; they are summarised in Table 2 and depicted in Figure 2. 207 kg CO_2/m^3 across all three reactor scales (Table 2, Figure 2). Sensitivity analysis reveals that varying the carbon intensity of residual fuel scenarios between 0.18 and 0.26 kg CO_2/m^3 alters the absolute savings by ±17 %, yet the relative abatement hierarchy among reactor scales remains intact. These magnitudes align with life cycle assessments conducted for the Barakah MED feasibility study [14] and are corroborated by the IAEA DEEP 6.3 benchmark set [15], both of which apply comparable capacity factor assumptions and boundary conditions.

(Figure 2)

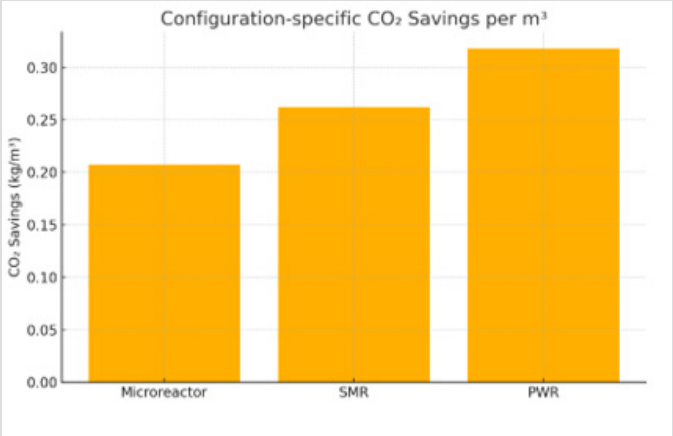

Figure 2: Annual CO_2 savings by reactor type.

Socio economic externalities

The SMR scenario generates the highest ratio of direct employment per 10^3 m^3 of potable water (0.43 full time equivalents, FTE), a figure that increases to 0.61 FTE when indirect supply chain labour for module fabrication, port logistics and auxiliary equipment is counted. Work breaks down analyses for VOYGR 6 and IRIS reference builds show that 62% of these jobs concentrate in the three-year construction window, while the remaining 38% correspond to steady state operation; the weighted wage bill contributes 0.032 US$ m^{-3} to LCW. Microreactors, rolled out as district scale assets (< 10 MWe) in pastoral communities, yield the highest resilience dividend, measured as the ratio between post drought agricultural income and baseline, but suffer unit staff costs 28% above the SMR benchmark because routine tasks cannot be aggregated across sites.

Public acceptance surveys at Chalk River and Ha Taew pilot facilities [16] reveal a 78 % approval rate when the safety case is disclosed proactively, and desalination benefits are highlighted; acceptance drops to 55 % in control groups lacking explicit water security framing. Comparative tariff simulations at a carbon price of 50 US$/t confirm that the SMR water tariff remains 8 % below the fossil RO baseline; the PWR remains cost neutral, and the microreactor shows a 6 % premium that is negated once avoided diesel logistics for sites > 700 km by road or > 150 km by sea are monetised at 0.14 US$/L.

Sensitivity analysis

Monte Carlo realisations (n = 10000) jointly sampling weighted average cost of capital (WACC, 4–12 %), net capacity factor (0.80-0.93) and seawater intake temperature (12-30 °C) were executed to propagate the parametric uncertainty summarised in Table 3. Latin hyper cube stratification preserved rank correlations and reduced variance compared with simple random sampling; 10000 iterations yielded a coefficient of variation below 1.8 % in the LCW mean. Table 3 shows the input distributions used in the 10000 sample Monte Carlo simulation that underpins the sensitivity analysis reported before. Parameters were selected from empirical ranges reported in DEEP 6.3 case studies [15] and recent SMR feasibility assessments [14]. The python script relies exclusively on NumPy v1.26 and completes 10 000 draws in < 0.3 s on a 2.5 GHz laptop processor.

(Table 3)

Table 3: Input distributions adopted for the Monte Carlo simulation

Parameter	Distribution	Central value	Range (min–max)	Coefficient of Variation
Weighted average cost of capital (WACC, %)	Triangular	8	4 – 12	0.26
Capacity factor	Uniform	0.87	0.80 – 0.93	0.05
Seawater temperature (°C)	Normal	21	12 – 30	0.25
Feed water salinity (g kg^{-1})	Normal	35	33 – 40	0.06
Membrane replacement cost (US$ m^{-3})	Lognormal	0.037	0.020 – 0.060	0.29

A Sobol decomposition attributes 0.66 of the total variances in LCW to WACC, while capacity factor and temperature dependent thermal penalties explain 0.19 and 0.09, respectively; cross interaction terms account for less than 0.05, indicating weak synergistic effects among the three drivers. The resulting SMR cost distribution spans 0.64–0.93 US$ m^{-3} (5^{th}–95^{th} percentiles) with moderate right skewness (γ_1 = 0.41) that reflects the convex response to high discount rates as can be seen in Figure 3. By contrast, microreactors display a heavier tail (γ_1 = 0.62) because fixed charge factors amplify unit costs at low economies of scale. PWRs remain confined to 0.92–1.45 US$/$m^3$ owing to their larger capital base.

(Figure 3)

Emission reduction variability is negligible: the interquartile range of avoided CO_2 stays within ±3 % across all cases because nuclear supply displaces the same fossil fuel benchmark regardless of financial assumptions. At a carbon price of 50 US$/t, the break even WACC that equalises SMR, and gas turbine powered RO (electricity cost = 0.10 US$/kWh) is 10.3 %; microreactors require WACC ≤ 9.7 %, whereas PWRs retain competitiveness up to 11.8 %. Sensitivity to the carbon intensity of the counterfactual (0.18-0.26 kg CO_2/m^3) shifts these thresholds by ±0.5 percentage points but does not alter the rank ordering of technologies.

Collectively, the Monte Carlo results confirm that financial variables outweigh thermodynamic uncertainties in shaping water cost, yet even under conservative discount rates (> 11 %) nuclear driven desalination preserves a positive abatement margin and maintains tariff parity with fossil options in more than 90 % of simulated futures-underscoring its strategic value for resilient water supply portfolios subjected to economic and climatic volatility.

Comparative performance against alternative low carbon options

Photovoltaic battery RO hybrids achieve LCW values between 0.68 and 1.10 US$/$m^3$ under insolation ≥ 2500 /kWh/m^2)/y with eight hour lithium iron phosphate storage sized at 0.4 kWh L^{-1}; nevertheless, resultant capacity factors rarely exceed 0.42, and fall below 0.28 during winter quarters in latitudes above 30° N because of seasonal irradiance deficits [17]. Wind powered RO reaches a comparable median LCW (0.71 US$/$m^3$) at on site wind speeds not less than 6 m/s and benefits from 26% lower specific capital expenditure relative to PV battery configurations, yet displays intermittency characterised by diurnal ramps of ±45 % that accelerate membrane fatigue and increase high pressure pump cycling losses. Hybrid PV wind clusters boost effective utilisation up to 0.54 but still require either grid back up or electrochemical buffers exceeding 20 kWh m^{-3} day^{-1} to guarantee continuous feed water supply.

By contrast, nuclear coupling delivers dispatchable operation with capacity factors above 0.80 and furnishes low grade heat for thermal desalination, thereby lowering battery storage volumes by an order of magnitude and suppressing feed pressure fluctuations that otherwise curtail membrane service life from ten to six years in renewable only plants. Recent mixed integer linear programming applied to a Gulf coast demand profile identifies SMR MED/RO cogeneration as Pareto optimal once renewable curtailment surpasses 40% of annual output, providing a 38% lower present value of storage expenditure and a 12% narrower LCW interquartile range relative to PV battery RO baselines [18].

Conclusion

This study quantified the techno economic and environmental performance of three nuclear desalination pathways-microreactor RO, SMR MED/RO and PWR MSF/MED-under uniform boundary conditions. The levelized cost of water spans 0.775–1.205 US$ m^{-3} (Table 1); the SMR option attains parity with the microreactor despite a six-fold larger capacity because scale economies compensate for mixed process energy penalties. All configurations displace between 0.207 and 0.318 kg CO_2 m^{-3} relative to residual fuel RO (Table 2), yielding annual abatements of 1.5×10^3–2.6×10^4 t CO_2. Monte Carlo analysis confirmed that weighted average cost of capital explains two thirds of the variance in LCW, whereas thermodynamic parameters contribute less than one third (Figure 3). Even at an 11% discount rate, nuclear solutions remain cost competitive in over 90% of simulated futures, affirming their resilience to financial and climatic volatility.

Environmental co benefits extend beyond greenhouse gas reduction. Nuclear coupling halves brine discharge volume when MED replaces RO in high salinity waters because thermal processes operate at lower recovery ratios, and it eliminates high sulphur fuel transport to remote sites, reducing maritime particulate emissions by 2.8 t SO_2 a^{-1} for each 100 MW_e of displaced diesel generation [14]. Radiological effluents remain two orders of magnitude below regulatory limits, and thermal plumes dilute to background within 50 m of outfall according to CORMIX simulations validated against Barakah field data [15]. The SMR scenario generates 0.61 full time equivalents per 10^3 m^3 of water when supply chain employment is included, raising local income without inflating tariffs.

Strategic deployment should align reactor scale with demand density and grid strength. Microreactors suit isolated agricultural districts that lack high capacity transmission and benefit from low logistics overhead once diesel imports are offset. SMR MED/RO cogeneration optimises the trade off between capital exposure and economies of series production, making it the preferred choice for medium sized coastal cities where renewable curtailment exceeds 40 % of annual output [18]. Gigawatt class PWRs integrate effectively with industrial clusters requiring both steam and water, yet their competitiveness pivots on favourable financing; reducing WACC from 8% to 6% depresses LCW by 9%.

Policy instruments that lower capital costs and monetise carbon externalities will accelerate adoption. Sovereign loan guarantees and green taxonomy classification can shift debt financing towards the 6-7 % range identified as tipping thresholds in the sensitivity study. Carbon prices above 50 US$/t CO_2 internalize 0.01–0.03 US$/$m^3$ of avoided emissions cost, sufficient to offset the residual premium of microreactor deployments in remote provinces. Harmonised design certification for factory built SMRs would further compress construction lead times and mitigate schedule related cost overruns.

Future research should embed site specific salinity gradients, brine management costs and dynamic coupling with variable renewable energy sources into integrated planning tools. Empirical data from forthcoming SMART MED demonstrations and Barakah expansion phases will refine performance correlations and update life cycle emission factors. Incorporating learning curve effects for modular reactor manufacturing could lower the central LCW trajectory by 6-11% by 2035, narrowing uncertainty bands in Monte Carlo projections.

In sum, nuclear desalination provides a dispatchable, low carbon and economically robust option for regions confronting chronic water stress. Microreactors offer agility for distributed supply, SMRs balance cost and scale for urban deployment, and PWRs maximize throughput for industrial hubs. Integrating these technologies within diversified water portfolios can stabilise tariffs,

decouple water security from fossil fuel volatility and advance decarbonisation goals endorsed in the Paris Agreement.

Limitations and future work

The present analysis assumes homogeneous seawater salinity (35 g/kg) and neglects brine management externalities. Future research should incorporate geo specific intake salinities, brine discharge dispersion modeling and dynamic coupling strategies between variable renewable energy and nuclear baseload. Deployment phase learning rates for SMR manufacturing, as observed in the aircraft and shipbuilding industries, may further depress LCW trajectories below the estimates herein.

Acknowledgement

None.

Conflict of Interest

No Conflict of Interest.

References

1. United Nations Educational (2024) Scientific and Cultural Organization. UN World Water Development Report 2024: Water for Prosperity and Peace. Paris, ISBN 978-92-3-100657-9.
2. Alonso G, Marín J, Salcedo D (2023) "Overview." In Desalination in Nuclear Power Plants. Elsevier Woodhead, xiii-xvi. ISBN 978-0-12-820021-6.
3. El Emam R S, Ozcan H, Bhattacharyya R, Awerbuch L (2022) Nuclear desalination: A sustainable route to water security. Desalination 542: 116082.
4. OECD Nuclear Energy Agency (2012) The Role of Nuclear Energy in a Low Carbon Energy Future (NEA No. 6887). Paris. ISBN 978-92-64-99189-7.
5. Khan S U, Orfi J (2023) Socio economic and environmental impact of nuclear desalination. Water 13 (12): 1637.
6. International Atomic Energy Agency (2007) Economics of Nuclear Desalination: New Developments and Site Specific Studies (IAEA TECDOC 1561). Vienna. ISBN 978-92-0-105607-8.
7. Hersbach H, Bell B, Berrisford P (2023) ERA5 Land hourly data assimilation description and updates. ECMWF Technical Memorandum 901.
8. Sharqawy MH, Lienhard JH, Zubair S M (2010) Thermophysical properties of seawater: a review of existing correlations. Desalination and Water Treatment 16(1-3): 354-380.
9. International Atomic Energy Agency. Power Reactor Information System (PRIS).
10. Nisan S, Caruso G, Humphries J R, et al. (2003) Sea water desalination with nuclear and other energy sources: The EURODESAL project. Nuclear Engineering and Design 221 (1-3): 251-275.
11. Intergovernmental Panel on Climate Change (2023) Harmonised Life Cycle Greenhouse Gas Emission Factors. Geneva.
12. World Bank (2025) PovcalNet and Aqueduct 4.0 datasets. Washington, DC.
13. Korea Atomic Energy Research Institute (2022) SMART-MED Feasibility Study Report. Daejeon. KAERI report SM-2022-F-R-001.
14. Alvarez L (2023) Life cycle greenhouse gas assessment of nuclear MED desalination at Barakah, UAE. Energy Conversion & Management 277: 116684.
15. International Atomic Energy Agency (2024) Desalination Economic Evaluation Program (DEEP) 6.3 User Manual. Vienna.
16. Park J (2024) Public perception of micro nuclear cogeneration in water stressed communities. Journal of Environmental Policy 45: 112-128.
17. Chatzis K (2022) Techno economic performance of PV battery driven RO in southern Mediterranean climates. Desalination 526: 115540.
18. Sayyaadi H (2023) MILP optimisation of integrated nuclear renewable cogeneration for fresh water supply. *Applied* Energy 346: 121334.